The EMBO Journal (2008) 27, 1085–1096 | © 2008 European Molecular Biology Organization | All Rights Reserved 0261-4189/08
www.embojournal.org

THE EMBO JOURNAL

Spindle assembly checkpoint gene *mdf-1* regulates germ cell proliferation in response to nutrition signals in *C. elegans*

Sonoko Watanabe, Takaharu G Yamamoto and Risa Kitagawa*

Department of Molecular Pharmacology, St Jude Children's Research Hospital, Memphis, TN, USA

When newly hatched *Caenorhabditis elegans* larvae are starved, their primordial germ cells (PGCs) arrest in the post-S phase. This starvation-induced PGC arrest is mediated by the DAF-18/PTEN–AKT-1/PKB nutrient-sensing pathway. Here, we report that the conserved spindle assembly checkpoint (SAC) component MDF-1/MAD1 is required for the PGC arrest. We identified 2 Akt kinase phosphorylation sites on MDF-1. Expression of a non-phosphorylatable mutant MDF-1 partially suppressed the defect in the starvation-induced PGC arrest in L1 larvae lacking DAF-18, suggesting that MDF-1 regulates germ cell proliferation as a downstream target of AKT-1, thereby demonstrating a functional link between cell-cycle regulation by the SAC components and nutrient sensing by DAF-18–AKT-1 during post-embryonic development. The phosphorylation status of MDF-1 affects its binding to another SAC component, MDF-2/MAD2. The loss of MDF-2 or another SAC component also caused inappropriate germ cell proliferation, but the defect was less severe than that caused by *mdf-1* hemizygosity, suggesting that MDF-1 causes the PGC arrest by two mechanisms, one involving MDF-2 and another that is independent of other SAC components.

The EMBO Journal (2008) **27,** 1085–1096. doi:10.1038/emboj.2008.32; Published online 28 February 2008
Subject Categories: cell cycle
Keywords: *C. elegans*; nutrition signals; spindle assembly checkpoint

Introduction

Caenorhabditis elegans are conceived as a single-cell zygote and undergo a nearly invariant developmental process that requires precisely controlled cell divisions. During development, the timing and axis of every round of cell division of each embryonic cell are regulated to follow the genetically programmed pattern (Sulston *et al*, 1983). Most cell divisions are completed during the first half of embryogenesis, within the proliferation phase, which lasts approximately 7 h after fertilization. The precursor cells of post-embryonic lineages become quiescent and stay dormant throughout the remainder of embryogenesis; cell-cycle progression then resumes after the larvae hatch under physiologically preferable conditions. Although being quiescent, many somatic precursors are blocked in the G1 stage in a cyclin-dependent kinase inhibitor (CKI-1)-dependent manner (Hong *et al*, 1998; Boxem and van den Heuvel, 2001). In contrast, two primordial germ cells (PGCs), Z2 and Z3, are arrested in early prophase (i.e., chromosomes with a 4N DNA content are highly condensed, but duplicated centrosomes are not yet separated into opposite poles) in a CKI-1-independent manner (Fukuyama *et al*, 2003, 2006).

In addition to genetically programmed cell-cycle control, environmental conditions cause global interruption of the reproducible pattern of cell division. For instance, when eggs hatch in the absence of food, larvae arrest early in the first larval stage (L1) and do not initiate post-embryonic development until food is restored (Baugh and Sternberg, 2006; Fukuyama *et al*, 2006; Kao *et al*, 2007). This dormant state is called L1 diapause. During L1 diapause, cell-cycle arrest of all somatic cells and germ cells is sustained (Hong *et al*, 1998; Baugh and Sternberg, 2006; Fukuyama *et al*, 2006). Fukuyama *et al* (2006) recently reported that *C. elegans* Pten, DAF-18, is required for maintenance of the cell-cycle arrest of PGCs during L1 diapause. PGCs in larvae homozygous for *daf-18* deletion (Δ*daf-18*) grown under nutritionally deprived conditions fail to arrest and continue dividing. DAF-18 is a negative regulator of insulin/insulin-like growth factor (IGF) pathway, which regulates biological processes such as dauer formation or longevity (Albert *et al*, 1981; Riddle *et al*, 1981; Dorman *et al*, 1995; Larsen *et al*, 1995; Ogg and Ruvkun, 1998; Gil *et al*, 1999; Rouault *et al*, 1999). The *C. elegans* insulin/IGF pathway is mediated by AGE-1/PI3K and AKT-1/-2 (Ogg and Ruvkun, 1998; Paradis and Ruvkun, 1998), as in other organisms (Vivanco and Sawyers, 2002). Consistent with DAF-18's function as a negative regulator of the insulin/IGF pathway, the inappropriate proliferation of germ cells in starved Δ*daf-18* larvae can be suppressed by the loss-of-function mutant of *age-1* or a deletion mutant of *akt-1* (Δ*akt-1*) (Fukuyama *et al*, 2006). Under nutritionally deprived conditions, DAF-18's phosphatase activity presumably antagonizes AGE-1 by dephosphorylating PIP_3, which transmits intracellular signals produced by AGE-1 kinase activity (Gil *et al*, 1999). Increased concentrations of PIP_3 activate a downstream kinase cascade that includes AKT-1/-2 (Ogg and Ruvkun, 1998; Paradis *et al*, 1999). DAF-18 thus regulates the germline checkpoint during L1 diapause by opposing the proliferation and growth-promoting activity of AKT-1 (Fukuyama *et al*, 2006). Although the structures of two *C. elegans* Akt kinases, AKT-1 and AKT-2, are highly related (Paradis and Ruvkun, 1998), inappropriate germ cell proliferation in starved Δ*daf-18* larvae is suppressed only by the

*Corresponding author: Department of Molecular Pharmacology, St Jude Children's Research Hospital, 332 N Lauderdale St Memphis TN 38105, USA. Tel.: +1 901 495 4058; Fax: +1 901 495 4290; E-mail: risa.kitagawa@stjude.org

Received: 3 September 2007; accepted: 8 February 2008; published online: 28 February 2008

Δ*akt-1* mutant but not by Δ*akt-2* (Fukuyama *et al*, 2006). Moreover, although Baugh and Sternberg recently reported that DAF-16, a forkhead-family transcription factor involved in the insulin/IGF pathway controlling the dauer formation and longevity (Gottlieb and Ruvkun, 1994; Lin *et al*, 1997; Ogg *et al*, 1997), is also required for the growth arrest of starved larvae in L1 (Baugh and Sternberg, 2006), the pathway controlling germline proliferation during L1 diapause does not require DAF-16 (Fukuyama *et al*, 2006). Thus, nutrient signal-dependent regulation of post-embryonic germline proliferation is controlled by the pathway that shares some common components with, but is distinct from, those involved in dauer formation and longevity. The downstream target of AKT-1 in the pathway controlling the germline proliferation during L1 diapause remains unknown.

The spindle assembly checkpoint (SAC) ensures proper chromosome segregation by delaying the metaphase–anaphase transition until every pair of sister chromatids in a cell is appropriately attached to the mitotic spindle; thus, the SAC maintains the genome stability of descendants. In response to an emergency signal from an unattached or tension-free kinetochore, the SAC prevents sister chromatids from separating by inhibiting the activity of a large ubiquitin ligase complex called the anaphase-promoting complex/cyclosome (APC/C^{CDC20}) (Musacchio and Salmon, 2007). Inactivation of APC/C^{CDC20} results in the accumulation of APC substrates such as the anaphase inhibitor securin (known as Pds1 in budding yeast) and cyclin B. The accumulation of securin inhibits the protease activity of separase, which is required for dissociation of sister chromatids from the centromeric region of mitotic chromosomes, whereas that of cyclin B prevents cells from exiting mitosis. As a consequence, the cell-cycle arrests take place before anaphase (Musacchio and Salmon, 2007).

SAC components Mad1-3, Bub1 and Bub3 were originally identified in budding yeast by 2 independent genetic screens (Hoyt *et al*, 1991; Li and Murray, 1991). Further study of these proteins revealed that they are structurally and functionally well conserved in eucaryotes (reviewed in Musacchio and Salmon, 2007).

In the SAC pathway, MAD2 binding to CDC20 is crucial, and efficient formation of the MAD2–CDC20 complex requires MAD1 (Luo *et al*, 2002). The molecular basis of MAD1's role in the SAC is thought to be that MAD1 forms a tight complex with a conformation of MAD2 known as closed-MAD2 (also known as C-MAD2 or N2-MAD2) and recruits a conformationally distinct MAD2, open-MAD2 (also known as O-MAD2 or N1-MAD2) to the unattached kinetochores, thereby facilitating the formation of the MAD2–CDC20 complex (Sironi *et al*, 2001, 2002; Luo *et al*, 2002). In this model, MAD1's localization to unattached kinetochores is a key step in SAC activation (Chen *et al*, 1998).

The *C. elegans* homologue of MAD1, MDF-1, has been identified as a binding partner of the *C. elegans* homologue of MAD2, MDF-2 (Kitagawa and Rose, 1999). Although MDF-1 has a relatively diverse amino-acid sequence, its predicted coiled-coil structure and the similarity between the short amino-acid sequence in the C-terminal domain with that of human MAD1 led us to categorize the protein as a member of the Mad1 protein family.

The *mdf-1*-deletion strain has various developmental defects (e.g., embryonic arrest, larval arrest, abnormal vulval development and sterility) (Kitagawa and Rose, 1999). These defects are comparable with phenotypes observed in worms depleted of either MDF-1 or MDF-2 by RNAi. Genome instability is reflected by the high incidence of males, which indicates the increased frequency of X-chromosome missegregation during meiosis. The presence of aneuploid oocytes also suggests that MDF-1 functions in the SAC. More direct evidence of the role of MDF-1 in the SAC in *C. elegans* is that MDF-1 is required for nocodazole-induced mitotic arrest of germ cells. Furthermore, Encalada *et al* (2005) recently demonstrated that, in embryonic cells, MDF-1 and MDF-2 are required for mitotic delays induced by chemical or mutational disruption of the microtubule cytoskeleton. Thus, MDF-1 and MDF-2 have an important function in the role of SAC in both embryonic cells and germ cells when mitotic spindle formation is compromised. However, depletion of MDF-1 or MDF-2 does not affect the mitotic duration under normal developmental conditions (Encalada *et al*, 2005), suggesting that SAC is not required for the normal timing of anaphase onset in early-stage embryos. Nevertheless, the loss of MDF-1 or MDF-2 causes severe defects in development and fertility.

Whether the role of MDF-1 in development and fertility is distinct from its function in the SAC remains unknown. However, the reduced-function mutations in APC/C^{CDC20} components such as *emb-30*(*APC4*) or *fzy-1*(*CDC20*) suppress the sterility caused by the loss of *mdf-1* (Furuta *et al*, 2000; Kitagawa *et al*, 2002; Tarailo *et al*, 2007); this finding suggests that MDF-1 regulates APC/C^{CDC20} activity to coordinate the timing of cell division for proper development. The mechanisms that regulate MDF-1's activity during development remain unknown.

Results and discussion

Hemizygosity of mdf-1 causes inappropriate germ cell proliferation during L1 diapause

In *C. elegans*, the loss of MDF-1 causes infertility, most likely due to severe defects in germline development. This finding suggests that MDF-1 regulates cell-cycle progression in germ cells. On that premise, we hypothesized that MDF-1 has a role in the cell-cycle arrest of PGCs during L1 diapause. To test this hypothesis, we first analysed germ cell proliferation in *mdf-1*(*gk2*)-deletion hemizygotes (Δ*mdf-1*/+) during L1 diapause. Newly hatched L1 larvae were starved for 4 days and then the number of PGCs per larva was counted. The body length of N2 (wild-type) worms did not increase during starvation, suggesting that their development was arrested in the L1 stage. The growth of Δ*mdf-1*/+ larvae was also retarded during starvation (Supplementary Figure S1). This growth retardation was reversible, and larval growth resumed after they were released from starvation (Supplementary Figure S1). The body length of the Δ*mdf-1*/+ larvae increased slightly during the first 24 h after hatching but did not change thereafter, even when the duration of starvation was extended to 5 days. Nevertheless, the majority (79%) of Δ*mdf-1*/+ larvae starved for 4 days contained more than four PGCs (Figure 1A and B). This finding contrasts with the strict limitation of 2–3 PGCs per N2 larva in response to nutrient-deprivation conditions, suggesting that inappropriate PGC proliferation occurs when the SAC is compromised (Figure 1A and B). Although the Δ*mdf-1*/+ strain exhibited

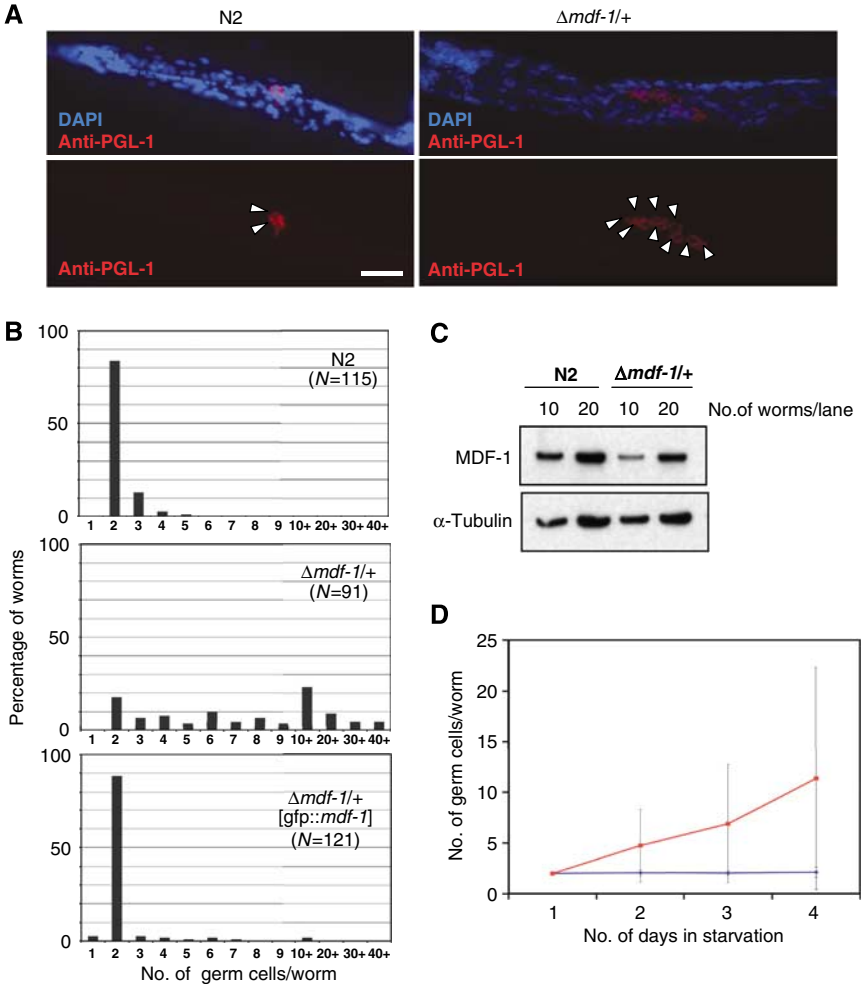

Figure 1 Hemizygosity of *mdf-1* causes a defect in starvation-induced cell-cycle arrest of PGCs. (**A**) Fluorescence micrographs of N2 (wild-type) and Δ*mdf-1*/+ worms in L1 diapause are shown. Newly hatched worms were starved for 4 days and then fixed. DNA was stained with DAPI (blue), and germ cell-specific P granules were stained with anti-PGL-1 antibody (red). Germ cells (PGL-1$^+$ cells) are indicated by white arrowheads. Scale bar, 15 μm. (**B**) Newly hatched worms of the indicated genotypes were starved for 4 days and then fixed. DNA and germ cell-specific P granules were stained with DAPI and anti-PGL-1 antibody, respectively. The number of PGL-1$^+$ cells per worm was counted, and the distribution of the number of germ cells per worm is plotted. (**C**) The level of MDF-1 expression in Δ*mdf-1*/+ larvae. Whole-worm lysates prepared from N2 or Δ*mdf-1*/+ larvae were separated on a gel, transferred to a nitrocellulose membrane and then probed with antibodies against MDF-1 and α-tubulin. The amount of lysate loaded into each well corresponded to that prepared from the indicated number of adult gravid worms. (**D**) The time course of germ cell proliferation during L1 diapause. N2 (blue plot) and Δ*mdf-1*/+ (red plot) larvae were hatched on NGM plates with no food, and a portion of each group of worms was then fixed every day for 4 days. Fixed worms were stained with DAPI and anti-PGL-1 antibody, and the germ cells were counted. The average number of germ cells per worm is plotted.

no significant defects in development or fertility (Kitagawa and Rose, 1999) western blot analysis using anti-MDF-1 antibody (Supplementary Figure S2) revealed that the level of MDF-1 expressed in Δ*mdf-1*/+ larvae was approximately 50% of that expressed in N2 larvae (Figure 1C). The defect in PGC arrest was also observed in starved L1 larvae that were hemizygous for *sDf29*, which deletes the *mdf-1* locus (Supplementary Figure S3). Moreover, we demonstrated that the expression of the GFP::MDF-1 fusion protein in Δ*mdf-1*/+ L1 larvae restored the starvation-induced arrest of PGCs in post-S phase (Figure 1B), indicating that inappropriate PGC proliferation is specifically caused by hemizygosity of *mdf-1*.

Inappropriate germ cell proliferation was also observed in maternally rescued L1 Δ*mdf-1* homozygotes starved for 4 days, but the frequency of larvae with more than three germ cells was only 30% (Supplementary Figure S4A). Thus, the defect in starvation-induced cell-cycle arrest of PGCs observed in Δ*mdf-1* homozygotes appeared to be less severe than that observed in Δ*mdf-1*/+ larvae. However, further characterization of PGCs arrested in Δ*mdf-1* homozygotes revealed that they failed to proliferate, regardless of the nutrition conditions. In contrast to N2 PGCs, which arrested during L1 diapause but resumed the cell-cycle progression when larvae were supplied with nutrients, the PGCs arrested in Δ*mdf-1* homozygotes remain undivided even 12 h after the larvae were released from starvation (Supplementary Figure S4B). These observations suggest that MDF-1 has a role not only in cell-cycle arrest of PGCs in response to nutrient deprivation, but also in the maintenance of the cells' ability to divide after being exposed to starvation conditions. These two roles are effective at different MDF-1 threshold levels: more MDF-1 is required for starvation-induced cell-cycle arrest than is required for germ cell

proliferation. Specifically, PGCs completely devoid of MDF-1 were irreversibly arrested under starvation conditions but with incomplete penetrance, and the arrested PGCs were unable to resume cell growth, even when the larvae were put back in nutrient-replete conditions. In this study, we focused on MDF-1 function in starvation-induced cell-cycle arrest, which is reversible, and characterized the phenotype of Δ*mdf-1* hemizygotes (instead of homozygotes) in most of the experiments.

To determine whether Δ*mdf-1/+* PGCs divide during embryogenesis or after hatching, we analysed the number of PGCs in newly hatched L1 larvae and in those starved for 1, 2 or 4 days after hatching. Time-course analysis revealed that the Z2 and Z3 cells in Δ*mdf-1/+* embryos remained undivided during late embryogenesis but started dividing upon hatching (Figure 1D). Therefore, halving the *mdf-1* gene dose did not affect the programmed entry into the post-S phase arrest during embryogenesis but did induce a defect in the ability of the larvae to sustain starvation-induced arrest of PGCs.

Because starvation-induced PGC arrest depends on a nutritional signal mediated by DAF-18 (Fukuyama *et al*, 2006), we next compared germ-line phenotypes of the Δ*mdf-1/+* strain with those of the strain homozygous for *daf-18*-deletion allele, *ok480* (Δ*daf-18*). Consistent with the previous report, the Δ*daf-18* strain exhibited defective cell-cycle arrest of PGCs (Figure 2). The Δ*daf-18* strain exhibited high phenotypic penetrance, that is, 97% of PGCs divided once or twice during L1 diapause, and 70% of the worms had 4–6 PGCs after 4 days of starvation (mean number of PGCs, 6.8 ± 2.44; variance, $\sigma^2 = 5.96$). In contrast, starved Δ*mdf-1/+* L1 larvae showed substantial intraindividual variability, that is, 21% of larvae had only 2–3 PGCs, and 25% had more than 10 PGCs (mean number of PGCs, 8.5 ± 5.31; variance, $\sigma^2 = 28.1$).

We also analysed the synthetic phenotype of the Δ*mdf-1/+*–Δ*daf-18* double mutant (Figure 2). The mean number of PGCs in the double-mutant larvae in L1 diapause was intermediate (7.5 ± 5.24), and the variance σ^2 was 27.45. Although our phenotypic analysis did not eliminate the possibility that MDF-1 activity is regulated independently of the DAF-18-controlled signalling pathway in response to nutritional signals, the synthetic phenotype was not additive, suggesting that MDF-1 function may not be completely independent of the DAF-18-mediated pathway.

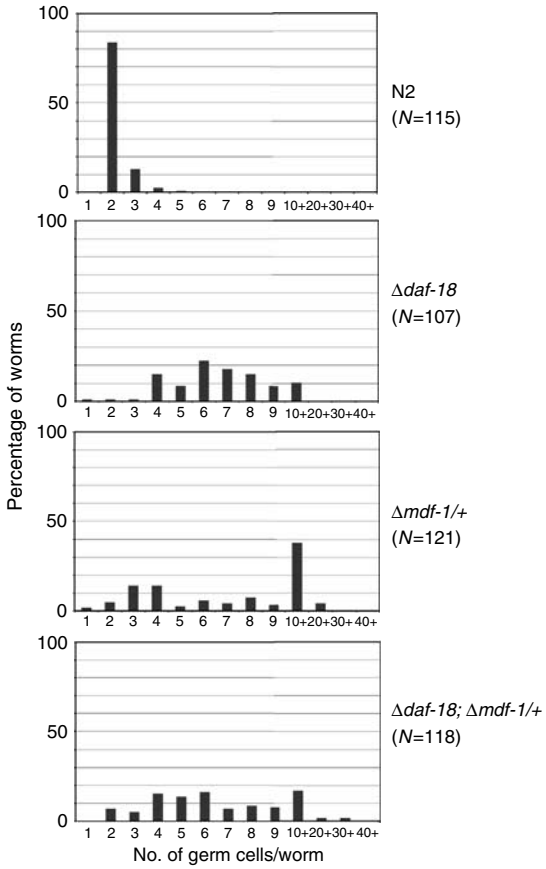

Figure 2 Inappropriate germ cell proliferation in Δ*mdf-1* hemizygotes and Δ*daf-18* homozygotes. Newly hatched worms of the indicated genotypes were starved for 4 days and then fixed. DNA and germ cell-specific P granules were stained with DAPI and anti-PGL-1 antibody, respectively. The number of PGL-1$^+$ cells per worm was counted, and the distribution of the number of germ cells per worm is plotted. Note that the plot of wild-type N2 data is a duplicate of the data shown in Figure 1B.

Hypomorphic mutant fzy-1 suppresses inappropriate germ cell proliferation

In the SAC pathway, Mad1 family proteins, including MDF-1, inhibit APC/C^{CDC20} activity in response to defects in microtubule-kinetochore attachment. Our previous finding that the lethality of Δ*mdf-1* homozygotes is suppressed by hypomorphic mutations in *emb-30*, a component of *C. elegans* APC/C, or in *fzy-1*, a *C. elegans* homologue of the substrate-specific APC/C activator CDC20, suggested that MDF-1 regulates APC/C^{CDC20} activity during development (Furuta *et al*, 2000; Kitagawa *et al*, 2002; Tarailo *et al*, 2007). We then questioned whether MDF-1-mediated inhibition of APC/C^{CDC20} is required for starvation-induced PGC arrest.

The hypomorphic mutant allele of *fzy-1*, *fzy-1*(*h1983*), suppresses the lethality of the Δ*mdf-1* homozygotes (Kitagawa *et al*, 2002). This allele has a missense mutation in the *fzy-1*-coding region that causes a single amino-acid alteration, that is, aspartic acid at residue 433 is substituted by asparagine. The FZY-1D433N mutant protein produced from the *fzy-1*(*h1983*) allele cannot bind the APC/C substrate IFY-1 (securin) (Kitagawa *et al*, 2002). In *fzy-1*(*h1983*)-mutant embryonic cells, the duration of mitosis of early-stage embryos is extended, presumably due to an increased level of IFY-1 (Tarailo *et al*, 2007).

We introduced the *fzy-1*(*h1983*) mutation into the Δ*mdf-1/+* strain and then analysed the germ cell proliferation in worms starved in L1 for 4 days. All of the *fzy-1* (*h1983*)–Δ*mdf-1/+* double-mutant larvae had only two or three germ cells (Figure 3). Thus, inappropriate germ cell proliferation caused by *mdf-1* hemizygosity was suppressed by the hypomorphic mutation in *fzy-1*. We also demonstrated that *emb-30*(*tn377*) mutation, which suppresses the lethality of the Δ*mdf-1* homozygotes at the permissive temperature (Furuta *et al*, 2000), also suppressed inappropriate germ cell proliferation caused by *mdf-1* hemizygosity (Supplementary Figure S5). These results suggest that MDF-1 has an important function in starvation-induced cell-cycle arrest of PGCs via its inhibition of APC/C activity.

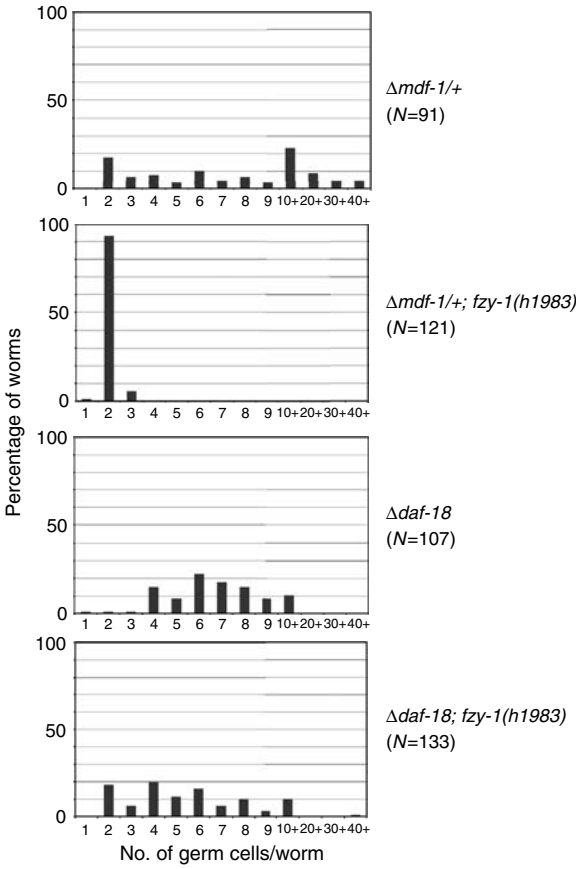

Figure 3 The *fzy-1*(*h1983*) hypomorphic allele of *fzy-1/CDC20* partially suppressed that caused by the loss of DAF-18. Newly hatched worms of the indicated genotypes were starved for 4 days and then fixed. DNA was stained with DAPI, and germ cell-specific P granules were stained with anti-PGL-1 antibody. The number of PGL-1^{+} cells per worm was counted, and the distribution of the number of germ cells per worm is plotted. Note that the charts of Δ*mdf-1/+* and Δ*daf-18* are duplicates of the data shown in Figures 1B and 2, respectively.

If MDF-1 and FZY-1 function downstream of DAF-18 in PGCs, then the *fzy-1*(*h1983*) mutant should also suppress inappropriate germ cell proliferation in the Δ*daf-18* strain. We generated *fzy-1*(*h1983*)–Δ*daf-18* double mutants and analysed their germ cell proliferation during L1 diapause. The *fzy-1*(*h1983*) mutant suppressed 18% of the defect in starvation-induced cell-cycle arrest of PGCs caused by the loss of DAF-18 (Figure 3). This result suggests that MDF-1–FZY-1 is, if not the sole target, a downstream factor of the signalling pathway that is negatively regulated by DAF-18.

MDF-1 is phosphorylated by AKT-1 kinase

DAF-18 is a negative regulator of the signalling pathway mediated by AGE-1 and AKT-1. However, which cell-cycle regulators are targets of this AGE-1–AKT-1 signalling pathway controlling nutrient signal-dependent germ cell proliferation remains unknown. Although our genetic analysis did not eliminate the possibility that MDF-1 regulates the germ cell proliferation independently of DAF-18, a finding that *fzy-1*(*h1983*), which suppresses the defect in starvation-induced cell-cycle arrest of PGCs caused by hemizygosity of *mdf-1*, also partially suppresses the defect caused by the loss of DAF-18 suggests that MDF-1 functions, in part, downstream of the AGE-1–AKT-1 signalling pathway. Therefore, we first hypothesized that MDF-1 activity is controlled by AKT-1-mediated phosphorylation.

Amino-acid sequence analysis of MDF-1 revealed 12 potential AKT kinase target sites ([R/K]XX[T/S]), including a perfect match with a consensus sequence for AKT phosphorylation sites (RXRXX[T/S]) (Alessi *et al*, 1996). Therefore, we wanted to determine whether MDF-1 is phosphorylated by AKT kinase *in vitro*. Bacterially expressed glutathione-*S*-transferase (GST) or GST-conjugated full-length MDF-1 (GST::MDF-1[1-679]) was incubated with purified human AKT kinase in the presence of [γ-^{32}P]ATP. A substantial amount of [γ-^{32}P]ATP was incorporated by GST::MDF-1; in contrast, none was incorporated by GST (Figure 4A and B), indicating that MDF-1 was phosphorylated by AKT *in vitro*.

To determine which sites on MDF-1 are AKT-1-phosphorylation targets, we generated GST-conjugated peptides containing 20 amino-acid peptide fragments of MDF-1 surrounding the potential phosphorylation sites as substrates for *in vitro* AKT kinase assay. A GST–GSK3β peptide served as a positive control and was efficiently phosphorylated by AKT kinase (Figure 4A and B). This assay identified two major phosphorylation sites, Thr523 and Thr672 (Figure 4C). We confirmed that Thr523 and Thr672 were phosphorylated by demonstrating that GST-conjugated peptides in which Thr523 and Thr672 were replaced with alanine did not incorporate [γ-^{32}P]ATP (Supplementary Figure S6).

The *akt-1*-null mutant suppresses inappropriate germ cell proliferation caused by the loss of DAF-18 (Fukuyama *et al*, 2006). This finding suggests that AKT-1 kinase is deregulated in Δ*daf-18* larvae. Therefore, we next tested whether the phosphorylation status of MDF-1 during L1 diapause is altered by the loss of DAF-18. Whole-worm lysate was prepared from Δ*daf-18* larvae and N2 larvae starved for 4 days in L1 diapause. The lysate was subjected to immunoprecipitation and western blot analysis. MDF-1 was immunoprecipitated with anti-MDF-1 antibody and then blotted with anti-phospho-Akt substrate antibody. The total amount of MDF-1 in Δ*daf-18* and N2 lysates was indistinguishable (Figure 4D). However, substantially more phosphorylated MDF-1 was detected in the MDF-1 pull-down from the Δ*daf-18* lysate than from the N2 lysate (Figure 4D).

The phosphorylation status of MDF-1 was also analysed in *akt-1*(*ok525*), an *akt-1*-null mutant (Δ*akt-1*), and in *akt-1*(*mg144*), a gain-of-function mutant allele (*akt-1gf*). The *akt-1*(*mg144*) allele can suppress the dauer-constitutive phenotype of *age-1*-null mutants (Paradis and Ruvkun, 1998), suggesting that AKT-1 is constitutively active in this mutant. Consistent with the previously proposed model that AKT-1 is inactivated in starved N2 larvae arrested in L1 presumably due to negative regulation by DAF-18 (Fukuyama *et al*, 2006), the amount of phosphorylated MDF-1 in the Δ*akt-1* lysate was indistinguishable from that in the N2 lysate. On the other hand, more phosphorylated MDF-1 was detected in the *akt-1gf* lysate (Figure 4D). In association with the increase in phosphorylated MDF-1, *akt-1gf* mutant larvae exhibited inappropriate germ cell proliferation during L1 diapause (Figure 4D). These results suggest that MDF-1 is phosphorylated in an *akt-1*-dependent manner during L1 diapause, when the AGE-1/PI3K–AKT-1/PKB signalling pathway is deregulated. A small but detectable amount of MDF-1 was

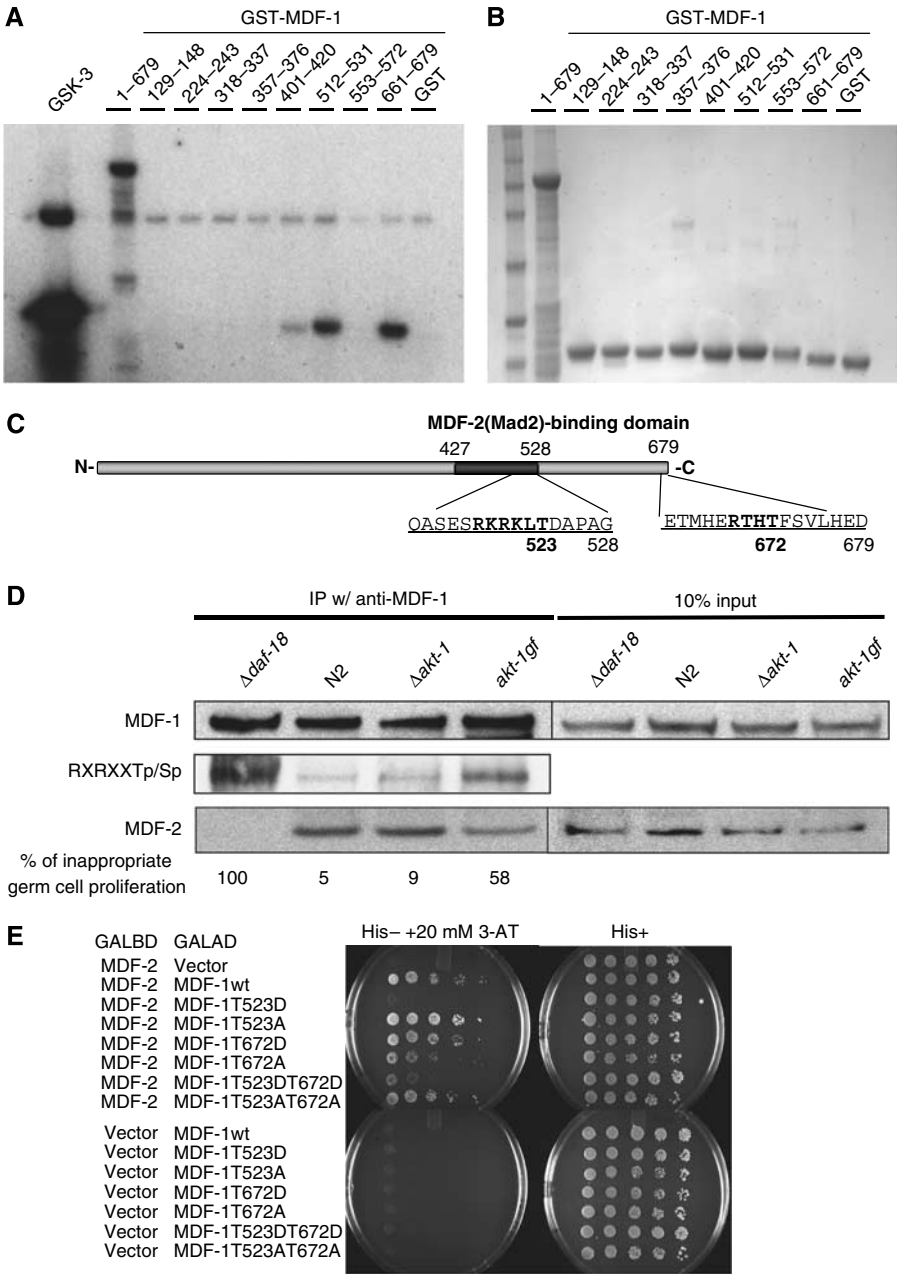

Figure 4 MDF-1 is phosphorylated at Thr523 and Thr672 *in vitro* in an AKT kinase-dependent manner. (**A**) Bacterially expressed GST protein and recombinant proteins consisting of fusions between GST and peptides derived from various regions of MDF-1 (the positions of the amino acids corresponding to each peptide are indicated) were purified with glutathione sepharose. Indicated proteins were incubated with Akt1 kinase and [γ-^{32}P]ATP at 30°C for 30 min, eluted with the SDS sample buffer, and separated on the gel. Incorporation of [γ-^{32}P]ATP was analysed by autoradiography. GSK-3 is a fusion protein containing the Akt1 phosphorylation motif of hGSK-3. (**B**) Indicated proteins, in the amount used in the Akt1 kinase reaction, were loaded, separated on the gel and then stained with Coomassie blue dye. (**C**) Schematic structure of MDF-1. The predicted MDF-2-binding domain is indicated by the dark grey bar. Consensus Akt kinase phosphorylation sites ([R/K]XX[T/S] or RXRXX[T/S]) present in peptides phosphorylated by Akt1 kinase *in vitro* are shown in bold letters. (**D**) Immunoprecipitations were performed using an affinity-purified anti-MDF-1 rabbit polyclonal antibody on extracts from L1 larvae of the indicated genotypes that had been starved for 4 days. The immunoprecipitants separated on a gel were transferred to the nitrocellulose membrane and then probed with phospho-Akt substrate-specific antibody (anti-RXRXXSp/Tp) or with anti-MDF-2 antibody. The probe was stripped, and then the membrane was reprobed with anti-MDF-1 antibody. (**E**) The yeast two-hybrid analysis was performed to test the binding activity of wild-type (MDF-1wt) or mutated MDF-1 proteins (MDF-1T523D, MDF-1T523A) to MDF-2. The yeast strain Y190 was transformed with the indicated combination of plasmid vectors, then the growth was analysed on agar plates of synthetic media that was −Leu, −Trp, (His +) or −Leu, −Trp, −His containing 20 mM 3-AT (His− + 20 mM 3-AT). Wild-type or mutant MDF-1 was cloned into the pACT vector, and MDF-2 was cloned into the pGBT9 vector. Vector: empty vector.

phosphorylated even in the absence of AKT-1. The amount of phosphorylated MDF-1 in Δ*akt-1* lysate was diminished when AKT-2 in Δ*akt-1* larvae was depleted by RNAi before starvation (Supplementary Figure S7), suggesting that MDF-1 is phosphorylated by both AKT-1 and AKT-2. Although AKT-2 is not required for nutrient signal-dependent germ cell proliferation control, MDF-1 may be phosphorylated by AKT-2 in other tissues.

AKT-1 deregulation hinders MDF-1 binding to MDF-2

Western blot analysis of MDF-1 immunoprecipitants with anti-MDF-2 antibody revealed that significantly less MDF-2 co-immunoprecipitated with MDF-1 in Δ*daf-18* lysate, and slightly less MDF-2 co-immunoprecipitated with MDF-1 in the *akt-1gf* lysate (Figure 4D). Thus, the increase in the phosphorylation of MDF-1 and the reduction of MDF-1 binding to MDF-2 correlates with the defect in starvation-induced cell-cycle arrest of germ cells caused by deregulation of AKT-1 activity by either gain-of-function mutations in *akt-1* or loss-of-function mutations in *daf-18* (Figure 4D). Therefore, we analysed whether the phosphorylation status of MDF-1 at Thr523 and/or Thr672 affects its ability to bind MDF-2. Phosphomimetic (Thr to Asp) or phosphorylation-disabled (Thr to Ala) mutations were introduced into Thr523 and/or Thr672 on MDF-1 to generate various MDF-1 mutants. MDF-2-binding activity of those mutants was tested by the yeast two-hybrid system. Consistent with the fact that Thr523 is located in the predicted MDF-2-binding domain (Jin *et al*, 1998) (Figure 4C), on the selection plate containing 20 mM 3-amino-1,2,4-triazole (3-AT), only the Thr523Asp mutation but not Thr523Ala exhibited substantially reduced binding (Figure 4E), suggesting that phosphorylation at Thr523 interferes with MDF-1 binding to MDF-2. In contrast, neither Thr672Asp nor Thr672Ala affected the MDF-1–MDF-2 interaction.

Non-phosphorylatable mutant MDF-1 partially suppresses the inappropriate germ cell proliferation caused by loss of DAF-18

The amount of phosphorylated MDF-1 correlates with the frequency of inappropriate germ cell proliferation. This finding led us to hypothesize that, in the absence of DAF-18, AKT-1 phosphorylates MDF-1, thereby inactivating MDF-1, which in turn leads to the failure of cell-cycle arrest of PGCs. To test this hypothesis, we constructed transgenic strains expressing either wild-type MDF-1 or non-phosphorylatable mutant MDF-1 (MDF-1Thr523AlaThr672Ala, hereafter referred to as MDF-1T523AT672A) fused with GFP in the Δ*mdf-1*–Δ*daf-18* background and then analysed germ cell proliferation during L1 diapause. The expression of both wild-type and mutant proteins suppressed the lethality of the Δ*mdf-1* homozygotes (data not shown). GFP::MDF-1 but not GFP::MDF-1T523AT672A in worm lysate prepared from starved L1

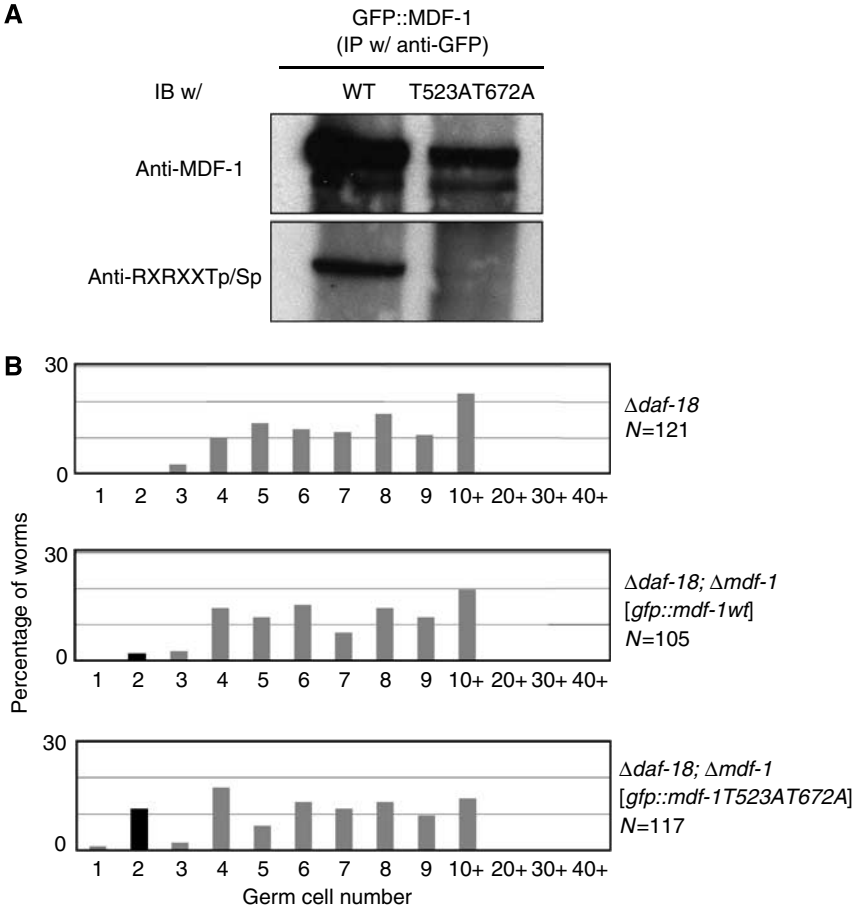

Figure 5 MDF-1T523AT672A partially suppressed the inappropriate germ cell proliferation caused by the loss of DAF-18. (**A**) Immunoprecipitations were performed using an anti-GFP rabbit polyclonal antibody on extracts from Δ*daf-18*, Δ*mdf-1* L1 larvae expressing either GFP::MDF-1(wild-type) or GFP::MDF-1T523AT672A that were starved for 4 days. The immunoprecipitants separated on a gel were transferred to the nitrocellulose membrane and then probed with anti-MDF-1 antibody or phospho-Akt substrate-specific antibody (anti-RXRXXSp/Tp). (**B**) Newly hatched worms of the indicated genotypes were starved for 4 days and then fixed. DNA and germ cell-specific P granules were stained with DAPI and anti-PGL-1 antibody, respectively. The number of PGL-1$^+$ cells per worm was counted, and the distribution of the number of germ cells per worm is plotted. The plots shown in black indicate the suppression of inappropriate germ cell proliferation.

larvae reacted with antibodies against the phosphorylated AKT substrate, suggesting that Thr523 and/or Thr672 are phosphorylated during L1 diapause *in vivo* (Figure 5A).

The expression of GFP::MDF-1 had little effect on the percentage of inappropriately proliferating germ cells. In contrast, the expression of GFP::MDF-1T523AT672A restored the cell-cycle arrest of germ cells in 12% of Δ*daf-18* larvae (Figure 5B). Thus, MDF-1T523AT672A partially suppressed the defect in starvation-induced PGC arrest caused by the loss of DAF-18. We can explain the incomplete suppression as follows: although the GFP fusion protein suppresses the lethality of Δ*mdf-1* homozygotes, it may not be fully functional, or the expression level of the GFP fusion protein by the *pie-1* promoter may not be sufficient for cell-cycle regulation of PGCs. Actually, the expression level of GFP::MDF-1 T523AT672A was lower than that of wild-type GFP::MDF-1 (Figure 5A). Alternatively, there may be other AKT-1 targets whose phosphorylation causes inappropriate germ cell proliferation. Our finding that the suppression effect of *fzy-1*(*h1983*), which completely suppresses the inappropriate germ cell proliferation caused by hemizygosity of *mdf-1*, on PGC proliferation in starved Δ*daf-18* larvae is partial (18%) also suggests the latter possibility.

Defective starvation-induced PGC arrest caused by the loss of other SAC components was less severe than that in mdf-1 hemizygotes

To determine whether germline quiescence during L1 diapause requires other SAC components, we analysed germ cell proliferation in *mdf-2*(*tm2190*)-deletion homozygotes (Δ*mdf-2*) and *san-1*(*ok1580*)-deletion homozygotes (Δ*san-1*). Unlike Δ*mdf-1* homozygotes, Δ*mdf-2* or Δ*san-1* homozygous strains are maintainable (Stein *et al*, 2007). Both strains exhibited slightly more inappropriate germ cell proliferation than that seen in N2 wild-type larvae (Supplementary Figure S8). However, their deficiency in cell-cycle arrest was much less severe than that observed in the Δ*mdf-1*/+ strain. Furthermore, the efficiency of the PGC arrest in the Δ*mdf-2*/+ strain resembled that of the N2 larvae (data not shown).

We analysed germ cell proliferation in mutants carrying alterations in alleles of other SAC genes that were isolated as mutants that suppress the 1-cell, embryonic-arrest phenotype of *mat-3*(*or180*), a hypomorphic allele of the gene encoding an APC/C component (Stein *et al*, 2007). Some alleles showed a slight increase in the frequency of inappropriate germ cell proliferation compared with their counterparts (Supplementary Figure S8). There was no apparent correlation between the severity of the defect in cell-cycle arrest of germ cells and the efficiency of suppression of the *mat-3*(*or180*) phenotype. Thus, although these results do not exclude the possibility that MDF-2 and SAN-1 are also required for proper germ cell quiescence during L1 diapause, because the defects in all of the other mutant alleles tested were not as severe as that observed in the Δ*mdf-1*/+ strain, we speculate that MDF-1 affects PGC proliferation by two independent mechanisms, one involving MDF-2 and another that is independent of other SAC components. However, in both cases, MDF-1 regulates the cell-cycle progression via inhibition of APC/C^{CDC20} activity.

APC/C^{CDC20} is thought to be inactivated by Emi1 during prophase for efficient accumulation of cyclins A and B, which are required for early mitotic progression (Reimann *et al*, 2001). Depletion of the SAC component BUB3 in *Drosophila* was recently shown to cause prolonged prophase (Lopes *et al*, 2005), suggesting that the SAC also inactivates the APC/C^{CDC20} for proper entry into mitosis. This finding shows the opposite outcome compared with ours in which MDF-1-mediated inhibition of the APC/C is required for starvation-induced cell-cycle arrest of germ cells at prophase (the early stage of mitosis). Therefore, different APC/C^{CDC20} substrates whose accumulation retains germ cells in prophase may be present. Although we found that IFY-1 (securin) accumulates in arrested PGCs (Supplementary Figure S9), whether IFY-1 regulates the G2/M transition or progression through prophase remains unknown.

MDF-1 controls germ cell proliferation in a cell-autonomous manner

We analysed the tissue-specific localization of MDF-1 in newly hatched L1-staged larvae. A substantial amount of MDF-1 was detected in PGCs (Supplementary Figure S10). MDF-1 accumulated not only in PGCs but also in intestinal cells (Supplementary Figure S10). To address whether MDF-1 functions cell autonomously or non-cell autonomously in PGCs, we performed RNAi experiments using *rrf-1* and *rrf-3* mutant strains. The *rrf-1* gene encodes an RNA-directed RNA polymerase (RdRP) homologue. Somatic cells (but not germ cells) carrying the homozygous *rrf-1*(*pk1417*) allele are resistant to RNAi treatment. The *rrf-3*(*pk1426*) is an *rrf-3*-null allele, and worms homozygous for *rrf-3*(*pk1426*) are hypersensitive to RNAi. When *mdf-1* was targeted by RNAi before nutrient deprivation, *rrf-1*(*pk1417*) worms as well as *rrf-3* (*pk1426*) worms exhibited more inappropriate germ cell proliferation during L1 diapause than did worms treated with control RNAi (Supplementary Figure S11). This result suggests that MDF-1 functions cell autonomously in PGCs. We also tried to resolve whether DAF-18 functions in PGCs cell autonomously or non-cell autonomously by performing the RNAi-targeting *daf-18* but failed because *daf-18* RNAi under our experimental condition could not phenocopy the inappropriate germ cell proliferation phenotype of Δ*daf-18* strain, even in the *rrf-3*(*pk1426*) strain.

MDF-1 ensures the quality of germ cells by sustaining PGC arrest under starvation conditions

We next questioned whether Δ*mdf-1*/+ germ cells, which inappropriately proliferated during L1 diapause, develop properly after release from starvation and resumption of larval growth. Newly hatched N2 or Δ*mdf-1*/+ L1 larvae were starved for 4 days and then transferred to plates containing bacteria as food. N2 PGCs that had arrested in post-S phase during starvation started dividing and kept proliferating during post-embryonic development. The ratio of fertilized eggs per N2 worm released from 4 days of starvation to that of N2 worms grown under the nutritionally preferable conditions was 96.7% (Figure 6A).

The Δ*mdf-1*/+ germ cells that inappropriately proliferated during starvation kept proliferating after the larvae were fed. However, the ratio of fertilized eggs per Δ*mdf-1*/+ worms released from starvation was 66.1% of that of Δ*mdf-1*/+ worms grown under the nutritionally preferable conditions (Figure 6A). Thus, the Δ*mdf-1*/+ germ cells that inappropriately proliferated during L1 diapause generated fewer viable zygotes, suggesting that starvation-induced cell-cycle arrest

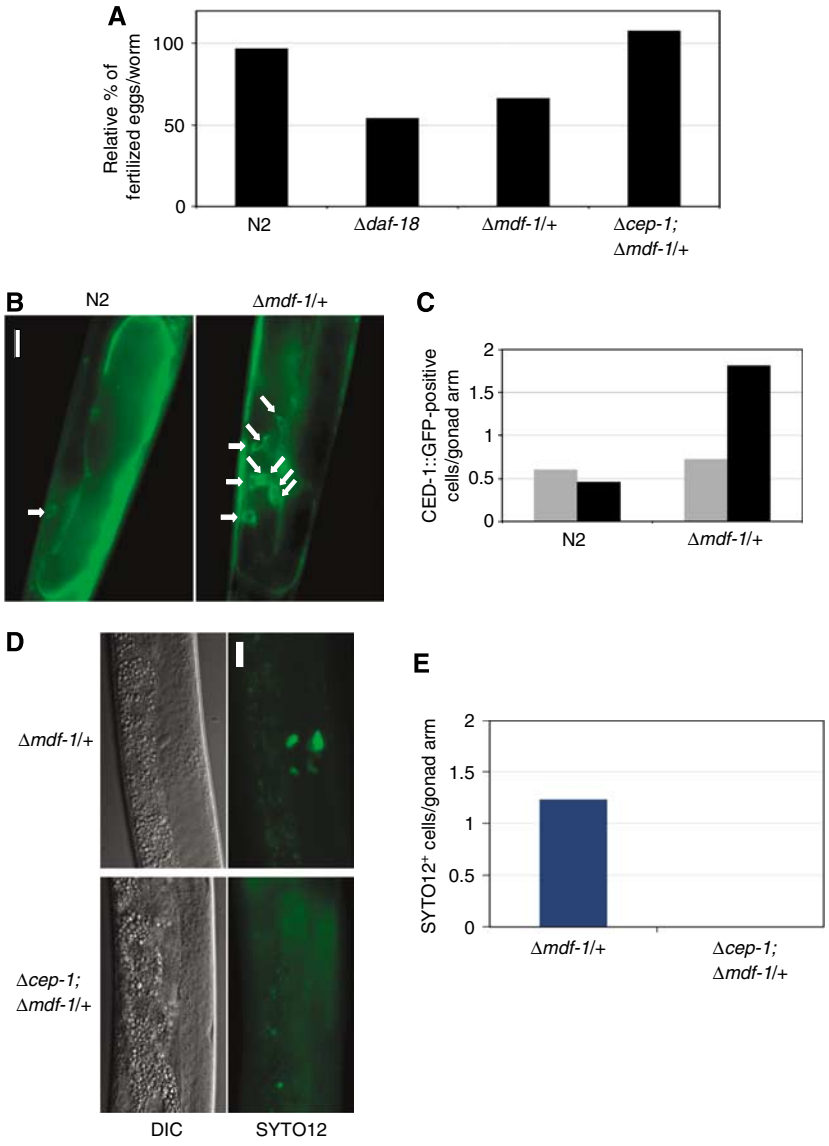

Figure 6 Germline apoptosis and reduction of brood size in *mdf-1* hemizygotes released from starvation are *cep-1* dependent. (**A**) Hermaphrodites of the indicated strains were grown in the presence of OP50 bacteria or starved for 4 days and then fed. The number of fertilized eggs laid per worm was counted for three individual worms, and the proportion of the fertilized eggs laid by temporarily starved worms compared with that laid by worms grown under normal conditions is shown. (**B**) Fluorescent microscope images of gonads of CED-1::GFP-expressing strains with indicated genetic backgrounds are shown. The worms were starved for 4 days and then fed for 2 days. Apoptotic cells surrounded by CED-1::GFP are indicated by white arrows. Scale bar, 15 μm. (**C**) The indicated strains were either grown for 2 days after hatching (pale grey bars) or starved for 4 days and then fed for 2 days (dark grey bars). The mean number of apoptotic cells per gonad arm of the indicated strains is plotted. (**D**) The differential interference contrast (DIC) microscope images (left panels) and fluorescent microscope images (right panels) of gonads of strains with the indicated genotypes stained with SYTO12 are shown. The newly hatched L1 larvae were starved for 4 days and then fed for 2 days. Apoptotic cells were positively stained with SYTO12. Scale bar, 15 μm. (**E**) The average numbers of SYTO12$^+$ cells per gonad arm in worms with the indicated genotypes are plotted.

of PGCs is required for maintenance of germ cell quality. We also analysed germ cells in the Δ*daf-18* strain, and the results were comparable with those seen with the Δ*mdf-1/+* strain (Figure 6A), thereby strengthening our argument that starvation-induced PGC arrest ensures the fertility of the animal under starvation conditions.

Mammalian embryonic cells lacking a functional SAC exhibit genomic instability and are targeted by the p53-dependent apoptotic pathway, presumably via activation of the DNA-damage checkpoint (Dobles *et al*, 2000; Baker *et al*, 2004; Baker *et al*, 2006). If MDF-1-dependent cell-cycle arrest of PGCs during L1 diapause is required for maintenance of the genome stability of germ cells, then Δ*mdf-1/+* germ cells inappropriately proliferated under starvation conditions should exhibit chromosome instability, and their descendants should be targeted as substrates for germline apoptosis.

We analysed germline apoptosis in transgenic strains expressing CED-1::GFP in the N2 or Δ*mdf-1/+* background. Germ cells undergoing apoptosis were easily detected because they were surrounded by CED-1::GFP (Zhou *et al*, 2001; Venegas and Zhou, 2007) (Figure 6B). Under the nutritionally preferable condition, the mean number of apoptotic cells per gonad arm of CED-1::GFP-expressing N2 worms was 0.61, and that of Δ*mdf-1/+* worms was 0.73 (Figure 6C). When newly hatched N2 worms were starved for 4 days and then fed for 2 days, the mean number of apoptotic

cells per gonad arm was 0.46 (Figure 6C). Thus, the 4-day starvation did not affect the frequency of germline apoptosis in the N2 background. In contrast, the mean number of apoptotic cells per gonad arm in the Δ*mdf-1/+* larvae maintained under the same conditions more than doubled to 1.81 (Figure 6C).

The introduction of *gk138*, a deletion allele of *cep-1, C.elegans* p53 (Δ*cep-1*) (Schumacher *et al*, 2001), completely suppressed the incidence of apoptotic cells in the gonad of starved Δ*mdf-1/+* larvae (Figure 6D and E). Furthermore, Δ*cep-1* suppressed the reduction in the brood size of Δ*mdf-1/+* worms released from starvation (Figure 6A). This finding supports our hypothesis that inappropriate germ cell proliferation caused by hemizygosity of *mdf-1* leads to genome instability in germline descendants, which are targeted as substrates for germline apoptosis, thereby leading to the reduction of viable zygotes. Thus, our results suggest that MDF-1 maintains the genome stability of germ cells by causing cell-cycle arrest in response to nutrition deprivation.

MDF-1 also has an important function in nutrient deprivation-induced somatic cell arrest

Although the body length of N2 L1 larvae remained unchanged during starvation, after a day of starvation, the body length of the Δ*mdf-1/+* larvae was slightly bigger than that of hatchlings (Supplementary Figure S12). This increase in body length may reflect the increased cell size or cell number in some somatic cells of post-embryonic lineage. To analyse the cell division of other somatic precursors of post-embryonic lineage, we counted the number of seam cells in transgenic strains expressing SCM::GFP in the N2 or Δ*mdf-1/+* background. The epidermal seam cells consist of 10 precursors, H0-2, V1-6 and T at the hatching stage. During the L2 stage, six of these cells undergo symmetrical division, resulting in the increase in the number of seam cells from 10 at L1 to 16 at L2 and beyond (Sulston and Horvitz, 1977). One hundred per cent of N2 larvae starved for 4 days after hatching had nine or ten SCM::GFP-positive cells. The intensity of the GFP signal in V5 cells was not sufficient for detection in some larvae; thus, nine GFP-positive cells were detected, indicating starvation-induced larval arrest in the L1 stage. We found some Δ*mdf-1/+* L1 larvae starved for 4 days bearing 9–10 SCM::GFP-positive cells, but others had more (range, 12–17 SCM::GFP-positive cells) (Supplementary Figure S12). These results suggest that the hemizygosity of *mdf-1* causes extra cell division of seam cell precursors during L1 diapause with an incomplete penetrance. This result is unexpected because seam cell division during post-embryonic development is regulated at the G1-S progression in a LIN-35/Rb, FZR-1/Cdh1 and CKI-1-dependent manner (Hong *et al*, 1998; Boxem and van den Heuvel, 2001; Fay *et al*, 2002; Fukuyama *et al*, 2003; Xia *et al*, 2007). Whether MDF-1 regulates G1-S progression of seam cell precursors as a target of AKT-1 remains to be investigated.

Conclusion

Taken together, the findings from this study have enabled us to propose a model in which PGC quiescence during L1 diapause is mediated by MDF-1 as a downstream factor in one branch of the DAF-18-regulated AGE-1–AKT-1 signalling pathway (Figure 7). Akt phosphorylation sites on MDF-1 and other MAD1 family members are surrounded by relatively diverse amino-acid sequences; a simple homology search did not reveal any corresponding sites on MAD1 proteins expressed in other species. However, two potential Akt phosphorylation sites are present on the MAD2-binding domain of human MAD1. Therefore, the mechanism by which Akt regulates MAD1 activity might be conserved in mammals. This report is the first to demonstrate that the SAC component MDF-1 is required for cell-cycle regulation of post-embryonic lineages in response to nutritional status. MDF-1-mediated inhibition of the cell-cycle in response to non-spindle/kinetochore defects should shed light on the roles of SAC components in multicellular organisms.

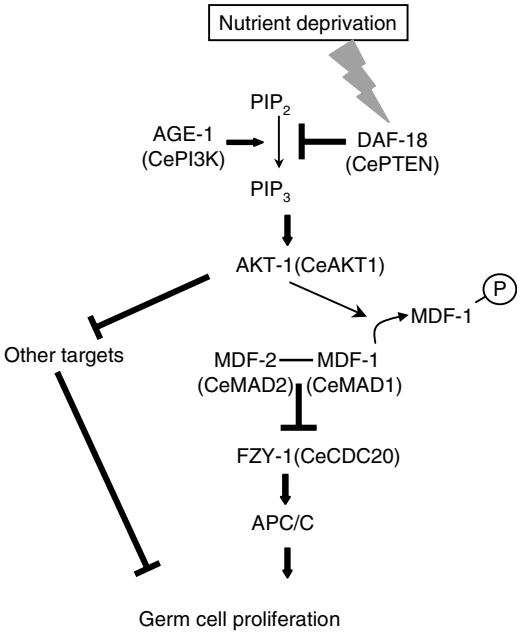

Figure 7 Proposed model of the pathway that controls germ cell proliferation during L1 diapause. MDF-1 causes the starvation-induced cell-cycle arrest of PGCs by inhibiting the activity of the APC/C^{CDC20}. MDF-1 is a downstream target of AKT-1. Phosphorylation of MDF-1 by AKT-1 reduces MDF-1's ability to bind MDF-2. DAF-18 indirectly activates MDF-1 by negatively regulating the AGE-1–AKT-1 signalling pathway. MDF-1–FZY-1 may not be the sole downstream factor of this pathway; another as yet unknown AKT-1 target may also regulate germ cell proliferation.

Materials and methods

C. elegans strains

Maintenance and cultivation of all strains were performed according to standard methods (Brenner, 1974). The strains were obtained from the Caenorhabditis Genetic Center (University of Minnesota, Minneapolis, MN) unless otherwise unregistered. Detailed description of the strains and their genotypes is available as Supplementary data at *The EMBO Journal* Online.

Maintaining worms in culture and counting germ cells

The preparation of starved worms and counting of germ cells were performed as described previously (Fukuyama *et al*, 2006), but with a minor modification. Starved worms were collected, fixed on glass slides and then stained with DAPI and anti-PGL-1 antibody (kindly provided by Susan Strome, Indiana University, Bloomington, IN). In some experiments using the *mdf-1*(*gk2*) heterozygotes (Δ*mdf-1/+* strains), fixed worms were stained with antibodies against MDF-1 and a component of germ cell-specific P granules to distinguish between Δ*mdf-1/+* ($MDF\text{-}1^{+}$) and Δ*mdf-1*-homozygous ($MDF\text{-}1^{-}$) L1 larvae.

Immunoprecipitation and western blot analyses

To prepare protein lysate from L1 diapause worms starved for 4 days, we suspended the worms in lysis buffer (75 mM HEPES (pH 7.5), 300 mM KCl, 1.5 mM $MgCl_2$, 1.5 mM EGTA, 15% glycerol, 0.05% NP-40, 1 mM DTT, protease inhibitors) and sonicated them with a Bioruptor UCD-200 (Diagenode Inc., Liege, Belgium). The lysate was cleared of worm debris by centrifugation.

MDF-1 immunoprecipitation was performed as follows: 1 μg anti-MDF-1 antibody and 10 μl wet volume of protein A-conjugated sepharose beads (GE Healthcare Bio-Sciences Corp., Piscataway, NJ) were added to 1 mg worm protein lysate. Protein–antibody complexes were precipitated, washed with lysis buffer and eluted with 2 × SDS sample buffer. Description of antibodies used for this study is available as Supplementary data at The EMBO Journal Online.

Akt1 phosphorylation assay

To fuse GST and MDF-1 proteins, we cloned PCR-amplified full-length cDNA of *mdf-1* or duplex oligonucleotides from various regions of *mdf-1* cDNA into the pACT-P*tac*-GST vector or pGEX4T-1 vector, expressed in BL21 cells, and purified with glutathione sepharose, as suggested by the manufacturer (GE Healthcare, UK). Purified proteins bound to sepharose beads were incubated with 400 ng Akt1 kinase (Upstate Millipore, Charlottesville, VA) and 10 μCi [γ-^{32}P]ATP at 30°C for 30 min in 20 μl Akt1 kinase buffer (20 mM HEPES (pH 7.4), 5 mM $MgCl_2$, 20 mM β-glycerophosphate, 1 mM EDTA, 0.1% β-mercaptoethanol). Phosphorylated proteins were eluted with 20 μl 2 × SDS sample buffer and then analysed by NuPAGE 4–12% Bis–Tris Gel (Invitrogen, Carlsbad, CA) and autoradiography. GST protein expressed in BL21 cells and purified with glutathione sepharose was used as the negative control for Akt1 kinase activity, and GSK-3 fusion protein (Cell Signaling Technology Inc., Danvers, MA) or GST–GSK-3 fusion protein generated in our laboratory was used as the positive control.

Yeast two-hybrid test

The yeast two-hybrid analysis was performed as described previously (Kitagawa and Abdulle, 2002). The yeast two-hybrid vectors pACT–MDF-1, pGBT9–MDF-2, pACT2 and pGBT9 were described previously (Kitagawa and Rose, 1999). The pACT–MDF-1T523A and pACT–MDF-1T523D were generated by replacing A1567 of *mdf-1* cDNA sequence with G for MDF-1T523A, and ACA from 1567 to 1569 with GAT for MDF-1T523D by *in vivo* site-directed mutagenesis using a three-fragment homologous recombination system (Kitagawa and Abdulle, 2002).

Germline apoptosis assay

Eggs from the CED-1::GFP-expressing strains, ZH231 *enIs7* [*Pced-1 ced-1*::gfp] and RQ263 *enIs7* [*Pced-1 ced-1*::gfp], and *mdf-1*(*gk2*)/*nT1* (Δ*mdf-1*/+) were isolated by the alkali/bleach method, seeded onto bacteria-free NGM plates, and incubated at room temperature for 12 h. L1 hatchlings were collected; half were transferred to NGM plates with OP50 bacteria and incubated for 2 days (not starved), and half were transferred to bacteria-free plates, incubated for 4 days, then transferred to NGM plates with OP50 bacteria and incubated for 2 days (starved). Worms were mounted under coverslips on glass slides in M9 medium containing 5 mM sodium azide. Their gonads were examined by fluorescence microscopy. Cells completely surrounded by CED-1::GFP were considered apoptotic. Approximately 40 gonads from each genotype were analysed. SYTO12 staining was performed as described (Gumienny *et al*, 1999).

Supplementary data

Supplementary data are available at *The EMBO Journal* Online (http://www.embojournal.org).

Acknowledgements

Some nematode strains were provided by the Caenorhabditis Genetics Center, which is funded by the NIH National Center for Research Resources (NCRR). These strains included deletion strains produced by the *C. elegans* Gene Knockout Consortium at the Oklahoma Medical Research Foundation and the University of British Columbia. We acknowledge Ann Rose, David Baillie and Zheng Zhou for providing strains, Susan Strome for kindly providing anti-PGL-1 polyclonal antibody, Andy Golden for providing strains and helpful suggestions for the manuscript, Iain Cheeseman and Arshad Desai for providing *C. elegans* GFP expression vector, pIC26, and Takao Fujisawa for assistance with construction of the double-mutant strains used for the genetic analysis. We thank Mary-Ann Bjornsti, Janet Partridge and Arshad Desai for their critical reading of the manuscript and members of St Jude Mitosis Club for many invaluable discussions and suggestions. This work was supported by the Cancer Center Support Grant CA021765 from the National Cancer Institute and by the American Lebanese Syrian Associated Charities (ALSAC).

References

Albert PS, Brown SJ, Riddle DL (1981) Sensory control of dauer larva formation in *Caenorhabditis elegans*. *J Comp Neurol* **198:** 435–451

Alessi DR, Caudwell FB, Andjelkovic M, Hemmings BA, Cohen P (1996) Molecular basis for the substrate specificity of protein kinase B; comparison with MAPKAP kinase-1 and p70 S6 kinase. *FEBS Lett* **399:** 333–338

Baker DJ, Jeganathan KB, Cameron JD, Thompson M, Juneja S, Kopecka A, Kumar R, Jenkins RB, de Groen PC, Roche P, van Deursen JM (2004) BubR1 insufficiency causes early onset of aging-associated phenotypes and infertility in mice. *Nat Genet* **36:** 744–749

Baker DJ, Jeganathan KB, Malureanu L, Perez-Terzic C, Terzic A, van Deursen JM (2006) Early aging-associated phenotypes in Bub3/Rae1 haploinsufficient mice. *J Cell Biol* **172:** 529–540

Baugh LR, Sternberg PW (2006) DAF-16/FOXO regulates transcription of cki-1/Cip/Kip and repression of lin-4 during *C. elegans* L1 arrest. *Curr Biol* **16:** 780–785

Boxem M, van den Heuvel S (2001) lin-35 Rb and cki-1 Cip/Kip cooperate in developmental regulation of G1 progression in *C. elegans*. *Development* **128:** 4349–4359

Brenner S (1974) The genetics of *Caenorhabditis elegans*. *Genetics* **77:** 71–94

Chen RH, Shevchenko A, Mann M, Murray AW (1998) Spindle checkpoint protein Xmad1 recruits Xmad2 to unattached kinetochores. *J Cell Biol* **143:** 283–295

Dobles M, Liberal V, Scott ML, Benezra R, Sorger PK (2000) Chromosome missegregation and apoptosis in mice lacking the mitotic checkpoint protein Mad2. *Cell* **101:** 635–645

Dorman JB, Albinder B, Shroyer T, Kenyon C (1995) The age-1 and daf-2 genes function in a common pathway to control the lifespan of *Caenorhabditis elegans*. *Genetics* **141:** 1399–1406

Encalada SE, Willis J, Lyczak R, Bowerman B (2005) A spindle checkpoint functions during mitosis in the early *Caenorhabditis elegans* embryo. *Mol Biol Cell* **16:** 1056–1070

Fay DS, Keenan S, Han M (2002) fzr-1 and lin-35/Rb function redundantly to control cell proliferation in *C. elegans* as revealed by a nonbiased synthetic screen. *Genes Dev* **16:** 503–517

Fukuyama M, Gendreau SB, Derry WB, Rothman JH (2003) Essential embryonic roles of the CKI-1 cyclin-dependent kinase inhibitor in cell-cycle exit and morphogenesis in *C. elegans*. *Dev Biol* **260:** 273–286

Fukuyama M, Rougvie AE, Rothman JH (2006) *C. elegans* DAF-18/PTEN mediates nutrient-dependent arrest of cell cycle and growth in the germline. *Curr Biol* **16:** 773–779

Furuta T, Tuck S, Kirchner J, Koch B, Auty R, Kitagawa R, Rose AM, Greenstein D (2000) EMB-30: an APC4 homologue required for metaphase-to-anaphase transitions during meiosis and mitosis in *Caenorhabditis elegans*. *Mol Biol Cell* **11:** 1401–1419

Gil EB, Malone Link E, Liu LX, Johnson CD, Lees JA (1999) Regulation of the insulin-like developmental pathway of *Caenorhabditis elegans* by a homolog of the PTEN tumor suppressor gene. *Proc Natl Acad Sci USA* **96:** 2925–2930

Gottlieb S, Ruvkun G (1994) daf-2, daf-16 and daf-23: genetically interacting genes controlling Dauer formation in *Caenorhabditis elegans*. *Genetics* **137:** 107–120

Gumienny TL, Lambie E, Hartwieg E, Horvitz HR, Hengartner MO (1999) Genetic control of programmed cell death in the

Caenorhabditis elegans hermaphrodite germline. *Development* **126:** 1011–1022

Hong Y, Roy R, Ambros V (1998) Developmental regulation of a cyclin-dependent kinase inhibitor controls postembryonic cell cycle progression in *Caenorhabditis elegans*. *Development* **125:** 3585–3597

Hoyt MA, Totis L, Roberts BT (1991) *S. cerevisiae* genes required for cell cycle arrest in response to loss of microtubule function. *Cell* **66:** 507–517

Jin DY, Spencer F, Jeang KT (1998) Human T cell leukemia virus type 1 oncoprotein Tax targets the human mitotic checkpoint protein MAD1. *Cell* **93:** 81–91

Kao G, Nordenson C, Still M, Ronnlund A, Tuck S, Naredi P (2007) ASNA-1 positively regulates insulin secretion in *C. elegans* and mammalian cells. *Cell* **128:** 577–587

Kitagawa K, Abdulle R (2002) *In vivo* site-directed mutagenesis of yeast plasmids using a three-fragment homologous recombination system. *Biotechniques* **33:** 288, 290, 292 passim

Kitagawa R, Law E, Tang L, Rose AM (2002) The Cdc20 homolog, FZY-1, and its interacting protein, IFY-1, are required for proper chromosome segregation in *Caenorhabditis elegans*. *Curr Biol* **12:** 2118–2123

Kitagawa R, Rose AM (1999) Components of the spindle-assembly checkpoint are essential in *Caenorhabditis elegans*. *Nat Cell Biol* **1:** 514–521

Larsen PL, Albert PS, Riddle DL (1995) Genes that regulate both development and longevity in *Caenorhabditis elegans*. *Genetics* **139:** 1567–1583

Li R, Murray AW (1991) Feedback control of mitosis in budding yeast. *Cell* **66:** 519–531

Lin K, Dorman JB, Rodan A, Kenyon C (1997) daf-16: An HNF-3/forkhead family member that can function to double the life-span of *Caenorhabditis elegans*. *Science* **278:** 1319–1322

Lopes CS, Sampaio P, Williams B, Goldberg M, Sunkel CE (2005) The *Drosophila* Bub3 protein is required for the mitotic checkpoint and for normal accumulation of cyclins during G2 and early stages of mitosis. *J Cell Sci* **118:** 187–198

Luo X, Tang Z, Rizo J, Yu H (2002) The Mad2 spindle checkpoint protein undergoes similar major conformational changes upon binding to either Mad1 or Cdc20. *Mol Cell* **9:** 59–71

Musacchio A, Salmon ED (2007) The spindle-assembly checkpoint in space and time. *Nat Rev* **8:** 379–393

Ogg S, Paradis S, Gottlieb S, Patterson GI, Lee L, Tissenbaum HA, Ruvkun G (1997) The Fork head transcription factor DAF-16 transduces insulin-like metabolic and longevity signals in *C. elegans*. *Nature* **389:** 994–999

Ogg S, Ruvkun G (1998) The *C. elegans* PTEN homolog, DAF-18, acts in the insulin receptor-like metabolic signaling pathway. *Mol Cell* **2:** 887–893

Paradis S, Ailion M, Toker A, Thomas JH, Ruvkun G (1999) A PDK1 homolog is necessary and sufficient to transduce AGE-1 PI3 kinase signals that regulate diapause in *Caenorhabditis elegans*. *Genes Dev* **13:** 1438–1452

Paradis S, Ruvkun G (1998) *Caenorhabditis elegans* Akt/PKB transduces insulin receptor-like signals from AGE-1 PI3 kinase to the DAF-16 transcription factor. *Genes Dev* **12:** 2488–2498

Reimann JD, Freed E, Hsu JY, Kramer ER, Peters JM, Jackson PK (2001) Emi1 is a mitotic regulator that interacts with Cdc20 and inhibits the anaphase promoting complex. *Cell* **105:** 645–655

Riddle DL, Swanson MM, Albert PS (1981) Interacting genes in nematode dauer larva formation. *Nature* **290:** 668–671

Rouault JP, Kuwabara PE, Sinilnikova OM, Duret L, Thierry-Mieg D, Billaud M (1999) Regulation of dauer larva development in *Caenorhabditis elegans* by daf-18, a homologue of the tumour suppressor PTEN. *Curr Biol* **9:** 329–332

Schumacher B, Hofmann K, Boulton S, Gartner A (2001) The *C. elegans* homolog of the p53 tumor suppressor is required for DNA damage-induced apoptosis. *Cutr Biol* **11:** 1722–1727

Sironi L, Mapelli M, Knapp S, De Antoni A, Jeang KT, Musacchio A (2002) Crystal structure of the tetrameric Mad1–Mad2 core complex: implications of a 'safety belt' binding mechanism for the spindle checkpoint. *EMBO J* **21:** 2496–2506

Sironi L, Melixetian M, Faretta M, Prosperini E, Helin K, Musacchio A (2001) Mad2 binding to Mad1 and Cdc20, rather than oligomerization, is required for the spindle checkpoint. *EMBO J* **20:** 6371–6382

Stein KK, Davis ES, Hays T, Golden A (2007) Components of the spindle assembly checkpoint regulate the anaphase-promoting complex during meiosis in *Caenorhabditis elegans*. *Genetics* **175:** 107–123

Sulston JE, Horvitz HR (1977) Post-embryonic cell lineages of the nematode, *Caenorhabditis elegans*. *Dev Biol* **56:** 110–156

Sulston JE, Schierenberg E, White JG, Thomson JN (1983) The embryonic cell lineage of the nematode *Caenorhabditis elegans*. *Dev Biol* **100:** 64–119

Tarailo M, Kitagawa R, Rose AM (2007) Suppressors of spindle checkpoint defect (such) mutants identify new mdf-1/MAD1 interactors in *Caenorhabditis elegans*. *Genetics* **175:** 1665–1679

Venegas V, Zhou Z (2007) Two alternative mechanisms that regulate the presentation of apoptotic cell engulfment signal in *Caenorhabditis elegans*. *Mol Biol Cell* **18:** 3180–3192

Vivanco I, Sawyers CL (2002) The phosphatidylinositol 3-Kinase AKT pathway in human cancer. *Nat Rev Cancer* **2:** 489–501

Xia D, Zhang Y, Huang X, Sun Y, Zhang H (2007) The *C. elegans* CBFbeta homolog, BRO-1, regulates the proliferation, differentiation and specification of the stem cell-like seam cell lineages. *Dev Biol* **309:** 259–272

Zhou Z, Hartwieg E, Horvitz HR (2001) CED-1 is a transmembrane receptor that mediates cell corpse engulfment in *C. elegans*. *Cell* **104:** 43–56

